Activation of extrasynaptic NMDA receptors induces a PKC-dependent switch in AMPA receptor subtypes in mouse cerebellar stellate cells

Lu Sun and Siqiong June Liu

Department of Biology, Penn State University, State College, PA 16802, USA

The repetitive activation of synaptic glutamate receptors can induce a lasting change in the number or subunit composition of synaptic AMPA receptors (AMPARs). However, NMDA receptors that are present extrasynaptically can also be activated by a burst of presynaptic activity, and thus may be involved in the induction of synaptic plasticity. Here we show that the physiological-like activation of extrasynaptic NMDARs induces a lasting change in the synaptic current, by changing the subunit composition of AMPARs at the parallel fibre-to-cerebellar stellate cell synapse. This extrasynaptic NMDAR-induced switch in synaptic AMPARs from GluR2-lacking (Ca^{2+}-permeable) to GluR2-containing (Ca^{2+}-impermeable) receptors requires the activation of protein kinase C (PKC). These results indicate that the activation of extrasynaptic NMDARs by glutamate spillover is an important mechanism that detects the pattern of afferent activity and subsequently exerts a remote regulation of AMPAR subtypes at the synapse via a PKC-dependent pathway.

(Resubmitted 17 May 2007; accepted after revision 15 June 2007; first published online 21 June 2007)
Corresponding author S. J. Liu: Department of Biology, 208 Mueller lab, Penn State University, State College, PA 16802, USA. Email: sjl16@psu.edu

Activity-induced enduring changes in the efficacy of synaptic transmission are thought to be a cellular mechanism underlying learning in the brain. It is well established that activation of postsynaptic NMDA receptors (NMDARs) allows Ca^{2+} entry via these receptors, inducing an homosynaptic change in the number or phosphorylation state of AMPA receptors (AMPARs) (Song & Huganir, 2002; Bredt & Nicoll, 2003). In many cases, NMDARs are also located some distance away from the synapse at extrasynaptic sites. These receptors can be activated by 'spillover' of glutamate during high-frequency presynaptic stimulation, and therefore this mechanism would be a good candidate for the encoding and storage of information of increased presynaptic activity.

Our previous studies revealed a new type of synaptic plasticity at the parallel fibre-to-cerebellar stellate cell synapse, in which Ca^{2+}-entry through GluR2-lacking AMPARs triggers the synaptic delivery of GluR2-containing receptors and the loss of GluR2-lacking receptors. This switch simultaneously reduces Ca^{2+} entry via AMPARs and alters the unitary conductance of the synaptic current (Liu & Cull-Candy, 2000, 2002, 2005). While this synaptic current is mediated solely by AMPARs, NMDARs are present at extrasynaptic sites on stellate cells and can be activated following high-frequency presynaptic stimulation (Carter & Regehr, 2000; Clark & Cull-Candy, 2002). Here we investigate whether activation of these NMDARs can alter the subunit composition of synaptic AMPARs.

Activity-dependent exchanges in AMPAR subtypes also occur at hippocampal synapses (Bagal *et al.* 2005; Thiagarajan *et al.* 2005) and have been implicated in ischaemia-induced neuronal death (Liu *et al.* 2004; Noh *et al.* 2005). Recent studies of the underlying molecular mechanism show that the activity-dependent insertion of GluR2-containing receptors requires a GluR2–PICK protein interacting with C-Kinase 1 interaction, while the loss of GluR2-lacking receptors involves disrupting their interaction with Glutamate receptor interacting protein (GRIP), which stabilizes the AMPARs at the synapse in stellate cells (Gardner *et al.* 2005; Liu & Cull-Candy, 2005). However the molecular mediator that links Ca^{2+} entry via glutamate receptors to the change in the relationship between AMPARs and their interacting partners is not known.

One link in this pathway may be protein kinase C (PKC). An activity-dependent intracellular Ca^{2+} rise can enhance the activity of this enzyme. Interestingly activation of PKC facilitates the targeting of PICK–GluR2 complexes

This paper has online supplemental material.

 DOI: 10.1113/jphysiol.2007.136788

to spines in hippocampal neurons (Perez *et al.* 2001), and is involved in the regulation of AMPAR trafficking during long-term depression (LTD) in hippocampal and Purkinje neurons and long-term potentiation (LTP) in dorsal horn neurons (Li *et al.* 1999; Daw *et al.* 2000; Xia *et al.* 2000; Kim *et al.* 2001). PKC phosphorylation of GluR2 disrupts the GluR2–GRIP interaction, and alters the AMPAR expression at synapses (Matsuda *et al.* 1999; Chung *et al.* 2000, 2003; Seidenman *et al.* 2003). Thus PKC is an ideal candidate to convert the Ca^{2+} signal into the exchange of synaptic AMPAR subtypes.

Here we tested the possibility that extrasynaptic NMDARs can function as a 'gate' or 'filter' that regulates under what conditions synaptic plasticity is induced. We show that activation of non-synaptic NMDARs can induce a lasting increase in GluR2-containing receptors and reduce the number of GluR2-lacking receptors at the parallel fibre–stellate cell synapse. This exchange of AMPAR subtypes requires the activation of PKC, and PICK drives the NMDAR-dependent delivery of GluR2-containing receptors.

Methods

Slice preparations

C57/BL6 mice (postnatal day 18–23) were used for these experiments. All experimental procedures were in accordance with the animal welfare guidelines of Penn State University. Following decapitation, cerebellar slices (250 μm) were obtained with a Leica VT1000S vibrating microslicer as previously described (Liu & Cull-Candy, 2000, 2005; Liu & Lachamp, 2006). Dissection and slicing of the cerebellum were performed in an ice-cold slicing solution (mM: 125 NaCl, 2.5 KCl, 0.5 $CaCl_2$, 7 $MgCl_2$, 26 $NaHCO_3$, 1.25 NaH_2PO_4, and 25 glucose, saturated with 95% O_2-5% CO_2, pH 7.4). Slices were maintained in external solution (identical to the slicing solution except that 0.5 mM $CaCl_2$ and 7 mM $MgCl_2$ were replaced with 2.5 mM $CaCl_2$ and 1 mM $MgCl_2$) at room temperature for 30–60 min before recording.

Electrophysiology

Whole-cell patch-clamp recordings were obtained using an Axoclamp 700A amplifier (Axon Instruments). Patch pipettes (4–7 MΩ) were filled with a Cs^+-based internal solution (mM: 140 CsCl, 2 NaCl, 10 CsHEPES, 0.5 or 10 CsEGTA, 4 Mg-ATP, 5 1 *N*-(2,6-dimethylphenylcarbamoylmethyl) triethyl ammonium bromide (QX314), 5 tetraethylammonium (TEA) and 0.1 spermine, pH 7.3). Series resistance and input resistance were 22.7 ± 0.7 MΩ ($n = 105$) and 819 ± 15 MΩ ($n = 24$), respectively.

Recordings were made from neurons located in the outer two-thirds of the molecular layer in cerebellar slices. Stellate cells were identified by the presence of spontaneous synaptic currents in the whole-cell configuration.

Synaptic currents. Spontaneous excitatory postsynaptic currents (sEPSCs) were recorded in an Mg^{2+}-free external solution or regular external solution (1 mM $MgCl_2$) that contained 100 μM picrotoxin (to block inhibitory synaptic currents) at various holding potentials (from −60 mV to +60 mV). No differences in the amplitude and rectification of sEPSCs were observed between the regular and Mg^{2+}-free external solutions (supplemental Table 1). When the Mg^{2+}-free solution was used, the slice in the recording chamber was continuously superfused by a gravity-fed system with the Mg^{2+}-free external solution for at least 30 min before recording. Recordings began 10–15 min after obtaining the whole-cell configuration (unless otherwise indicated), and usually lasted for a period of about 2 h. Series resistance was monitored every 5 min throughout the experiment, which was terminated if the value changed by more than 30%.

Stimulation of parallel fibres. The parallel fibres (PFs) in horizontal or coronal slices were stimulated by a train of depolarizations to cause 'spillover' of glutamate, which can activate non-synaptic NMDARs. A parallel bipolar electrode (150 μm spacing) was placed across the molecular layer about 200 μm from the recording electrode to stimulate PF inputs. The stimulus intensity was above threshold and ranged from 10 to 50 V with a stimulus duration of 100–200 μs. The stimulation protocol contained 100 sweeps of four depolarizations at 50 Hz, with a 2 s interval between two sweeps and 20 s between every 10 sweeps. PFs were stimulated in an external solution that contained 50 μM glycine, 1 μM strychnine, and 50 μM GYKI 52466. Experiments were performed at 32°C in regular external solution containing 1 mM $MgCl_2$ (further temperature elevation led to stability problems in these long-term recordings). During PF stimulation, the cell was voltage clamped at −70 mV and depolarized to 0 mV for 1 ms immediately after each burst stimulation. The brief depolarization was designed to mimic an action potential occurring in the postsynaptic cell that had been evoked by the presynaptic stimulation, and to remove the Mg^{2+} block of NMDA receptors. A few experiments were conducted in a Mg^{2+}-free external solution at room temperature, in which the postsynaptic cell was voltage clamped at −60 mV during PF stimulation (five depolarizations at 50 Hz) without a postsynaptic depolarization. In the experiment shown in Fig. 1, an extracellular glass stimulating electrode filled with ACSF was placed about 100 μm from the recording electrode in the molecular layer. The stimulation intensity was near threshold. A pipette solution containing 10 mM EGTA was used for all PF stimulation experiments.

Application of NMDA and glycine. To briefly activate NMDARs, 20 μM NMDA plus 50 μM glycine was applied by a double-barrelled gravity-fed perfusion system positioned just above the slice for 3 min while the stellate cell was voltage-clamped at −30 mV. We tested two pipette solutions (containing 0.5 or 10 mM EGTA) and observed no difference in the amplitude of sEPSCs (supplemental Table 1) and in the NMDA/glycine-induced change in

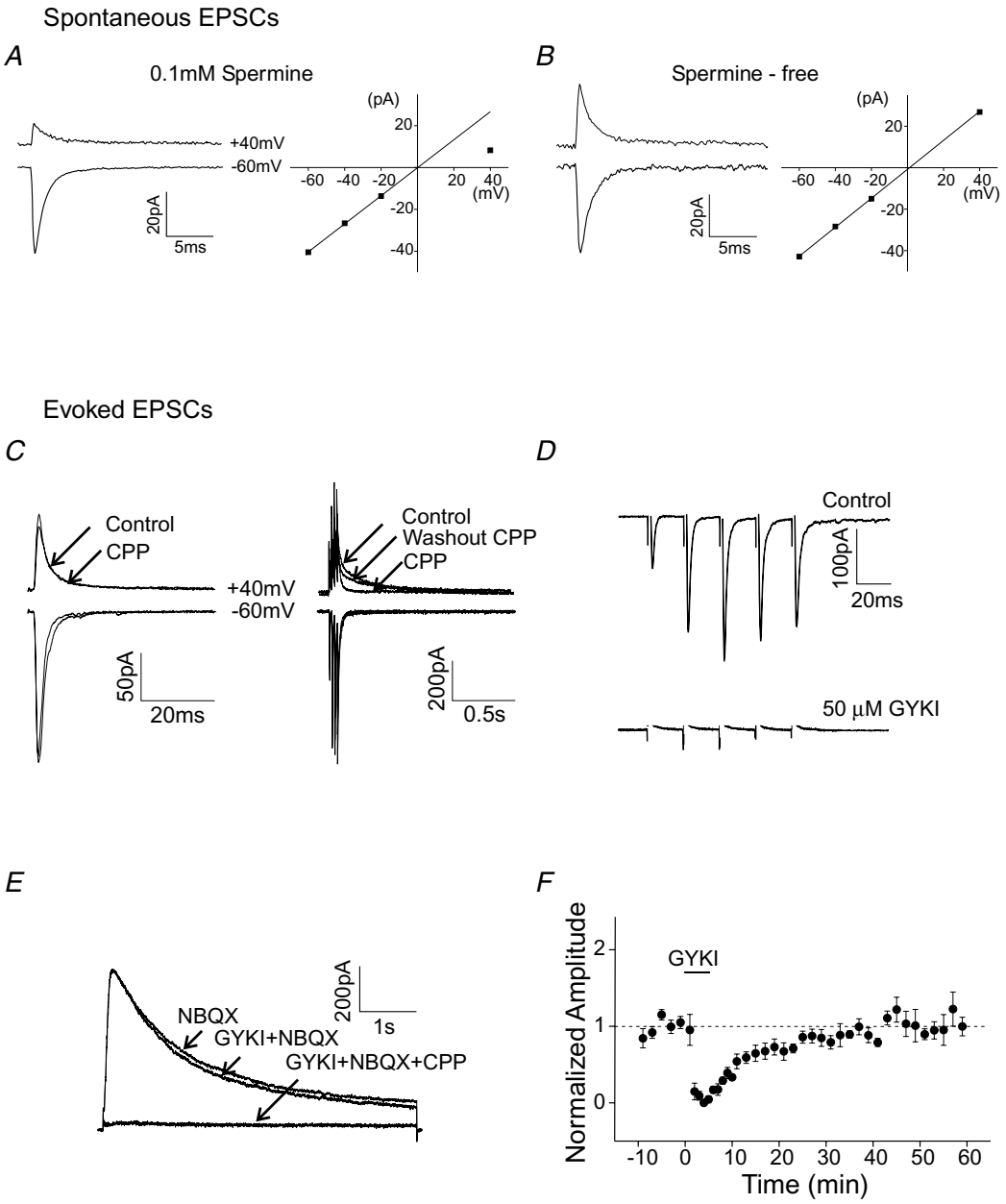

Figure 1. Characterization of glutamate receptor mediated synaptic and extrasynaptic currents in stellate cells

A, spontaneous EPSCs in stellate cells exhibit a reduced amplitude at +40 mV and inwardly rectifying *I–V* relationship when spermine is included in the pipette solution. *B*, synaptic currents recorded in the absence of spermine display a linear *I–V* relationship. *C–F*, GYKI 52466 reversibly inhibited the AMPAR-mediated synaptic current, but not the extrasynaptic NMDAR current evoked by a burst of high-frequency stimulation of parallel fibres using near-threshold stimulation intensity. The pipette solution did not contain spermine. *C*, EPSCs at −60 mV and +40 mV evoked by stimulation of parallel fibres with a single depolarization (left) and with a train of five depolarizations at 50 Hz (right). *D*, the effect of GYKI 52466 (50 μM) on AMPAR-mediated synaptic currents evoked by PF stimulation (five depolarizations at 50 Hz) in the presence of 20 μM CPP. Current traces at −70 mV. *E*, the extrasynaptic NMDAR-mediated current at +40 mV evoked by PF stimulation (five depolarizations at 50 Hz) in the presence of 10 μM NBQX. 50 μM GYKI 52466 and 20 μM CPP were bath applied. *F*, group data of sEPSC amplitude (normalized to the amplitude prior to the application of GYKI 52466) *versus* time ($n = 4$). These recordings were made in the regular ACSF that contained 1 mM Mg^{2+}.

the rectification of sEPSCs. Thus the pipette solution that contained 0.5 mM EGTA was used for the chemical induction experiments (unless otherwise stated). The experiments testing PKC inhibitors and agonists were performed in a Mg^{2+}-free external solution.

Analysis. Spontaneous EPSCs were filtered at 2 kHz and digitized at 20 kHz. The average current trace at each holding potential (typically 20–40 sEPSCs) was constructed by aligning each event on its point of fastest rise using N version 4.0 (written by Steve Traynelis, Emory University). Events that did not have smooth rise and decay phases were rejected. The current amplitude was plotted at each potential producing an *I–V* relationship. The mean sEPSC amplitudes at negative potentials were fitted by linear regression. The rectification index of the *I–V* relationship was defined as the ratio of the current amplitude at +40 mV to the predicted linear value at +40 mV (extrapolated from linear fitting of the currents at the negative potentials).

All values are expressed as mean ± S.E.M. Statistical significance was assessed using a two-tailed Student's *t* test. NMDA, GYKI 52466, R-CPP (4-(3-phosphonopropyl)piperazine-2-carboxylic acid), chelerythrine, pep2-AVKI and pep2-SVKE were obtained from Tocris, glycine and picrotoxin from Sigma, PKCI 19-36 from EMD Biosciences, and (–)indolactam-V and (+)indolactam-V from Alexis Biochemicals.

Results

To determine the subunit composition of synaptic AMPARs, spermine (0.1 mM) was included in the pipette solution. Spermine confers a voltage-dependent block to GluR2-lacking receptors producing an inwardly rectifying current–voltage (*I–V*) relationship, whereas AMPARs that contain GluR2 subunits display a linear *I–V* relationship (Bowie & Mayer, 1995; Kamboj *et al.* 1995; Koh *et al.* 1995; Washburn *et al.* 1997). Spontaneous EPSCs (sEPSCs) were recorded from stellate cells in a cerebellar slice at different holding potentials using the whole-cell voltage-clamp technique. Consistent with previous reports (Gardner *et al.* 2005; Liu & Cull-Candy, 2005), the amplitude of synaptic currents was smaller at depolarized potentials, compared with currents at hyperpolarized potentials (Fig. 1*A*, left). A plot of the amplitude of sEPSCs against the membrane potential showed an inwardly rectifying *I–V* relationship, indicating that GluR2-lacking receptors are present at the synapse (Fig. 1*A*, right). As a control in the absence of spermine, synaptic currents showed a linear *I–V* relationship ($n = 4$, Fig. 1*B*).

Stellate cells receive glutermatergic excitatory inputs from the axons of granule cells (parallel fibres). *In vivo* recordings of cerebellar granule cells show that sensory stimulation evokes a burst of action potentials at ∼80 Hz (Chadderton *et al.* 2004). While the synaptic current at the parallel fibre-to-stellate cell synapse is mediated solely by AMPARs, stimulation of parallel fibres with paradigms that resemble physiological stimulation can activate extrasynaptic NMDARs and presynaptic NMDARs on stellate cells (Glitsch & Marty, 1999; Carter & Regehr, 2000; Clark & Cull-Candy, 2002; Liu & Lachamp, 2006). We directly tested whether activation of extrasynaptic NMDARs by stimulating parallel fibres could alter the subtype of AMPARs at the synapse, i.e. whether the receptors switch from being Ca^{2+} permeable to Ca^{2+} impermeable.

Presynaptic stimulation activates extrasynaptic NMDARs and triggers a switch in AMPAR subtypes at the synapse

We first confirmed that although near-threshold stimulation of parallel fibres (PFs) with a single depolarization gave rise to a synaptic current that lacked an NMDA component (Fig. 1*C*, left), a burst of five depolarizations at 50 Hz evoked a current with a slow rise and decay time at +40 mV. This current was inhibited by 20 μM CCP, an NMDAR blocker (Fig. 1*C*, right). Thus, functional NMDARs are predominantly located at extrasynaptic sites and can be activated by the spillover of glutamate during high-frequency stimulation of presynaptic terminals. Thus, burst stimulation at 50 Hz was then used to activate extrasynaptic NMDARs.

We have previously demonstrated that activation of synaptic Ca^{2+}-permeable AMPARs is sufficient to induce the switch in AMPAR subtypes (Liu & Cull-Candy, 2000). To determine whether activation of extrasynaptic NMDARs can also alter the subunit composition of AMPARs at the synapse, we blocked AMPARs with GYKI 52466 during bursts of PF stimulation.

First, we determined the concentration of GYKI 52466 that blocked AMPAR-mediated synaptic currents but had minimal effects on the NMDAR-mediated current. In the presence of CPP, the synaptic current evoked by a train of PF stimulations was completely blocked by 50 μM GYKI 52466 (Fig. 1*D*). The addition of GYKI 52466 at this concentration did not inhibit NMDAR currents measured at +40 mV in the presence of NBQX, a non-NMDAR antagonist (Fig. 1*E*).

Second, we determined the washout time that was required to fully reverse the inhibition of AMPARs by GYKI 52466. Spontaneous EPSCs (sEPSCs) were measured prior to application of GYKI 52466 and during its washout with artificial cerebrospinal fluid (ACSF). The amplitude of sEPSCs returned to the control level within 30 min of washout (Fig. 1*F*). Therefore GYKI 52466 (50 μM) was added 2 min before stimulation to block AMPARs, and parallel fibres were then stimulated to activate extrasynaptic NMDARs (Fig. 2*A*). Following the

PF stimulation, GYKI 52466 was removed by continuous washout with ACSF for 30 min.

Third, we tested whether stimulating the PFs with a depolarizing train followed by a brief depolarization of the postsynaptic cell to 0 mV from −70 mV could effectively remove the Mg^{2+} block of the postsynaptic NMDARs. The brief depolarization was designed to mimic an action potential occurring in the postsynaptic cell that had been evoked by the presynaptic stimulation. This stimulation protocol evoked an inward NMDAR current in ACSF (containing 1 mM Mg^{2+}) that was 83 ± 14% (measured as charge transfer; $n = 8$) of that observed when the postsynaptic cell was voltage clamped at −30 mV. A smaller current was observed when the postsynaptic cell was not briefly depolarized (43 ± 15%; $n = 7$; $P < 0.05$; see supplemental Fig. 1). The charge transfer of the NMDAR-EPSCs evoked by PF stimulation followed by a brief depolarization was ∼42% of the total NMDAR-EPSC charge in the Mg^{2+}-free condition, using a similar stimulation intensity (Fig. 3*A*). This stimulation protocol thus partially removes the Mg^{2+} block and was used to activate NMDARs in the presence of Mg^{2+}. The weak blockade of the NMDAR current by Mg^{2+} is probably due to the expression of NMDARs that contain NR2D subunits, since these have a low Mg^{2+} sensitivity (Momiyama *et al.* 1996). Stellate cells are known to express this subunit (Akazawa *et al.* 1994; Thompson *et al.* 2000). The size of the NMDAR-EPSC in the Mg^{2+}-free

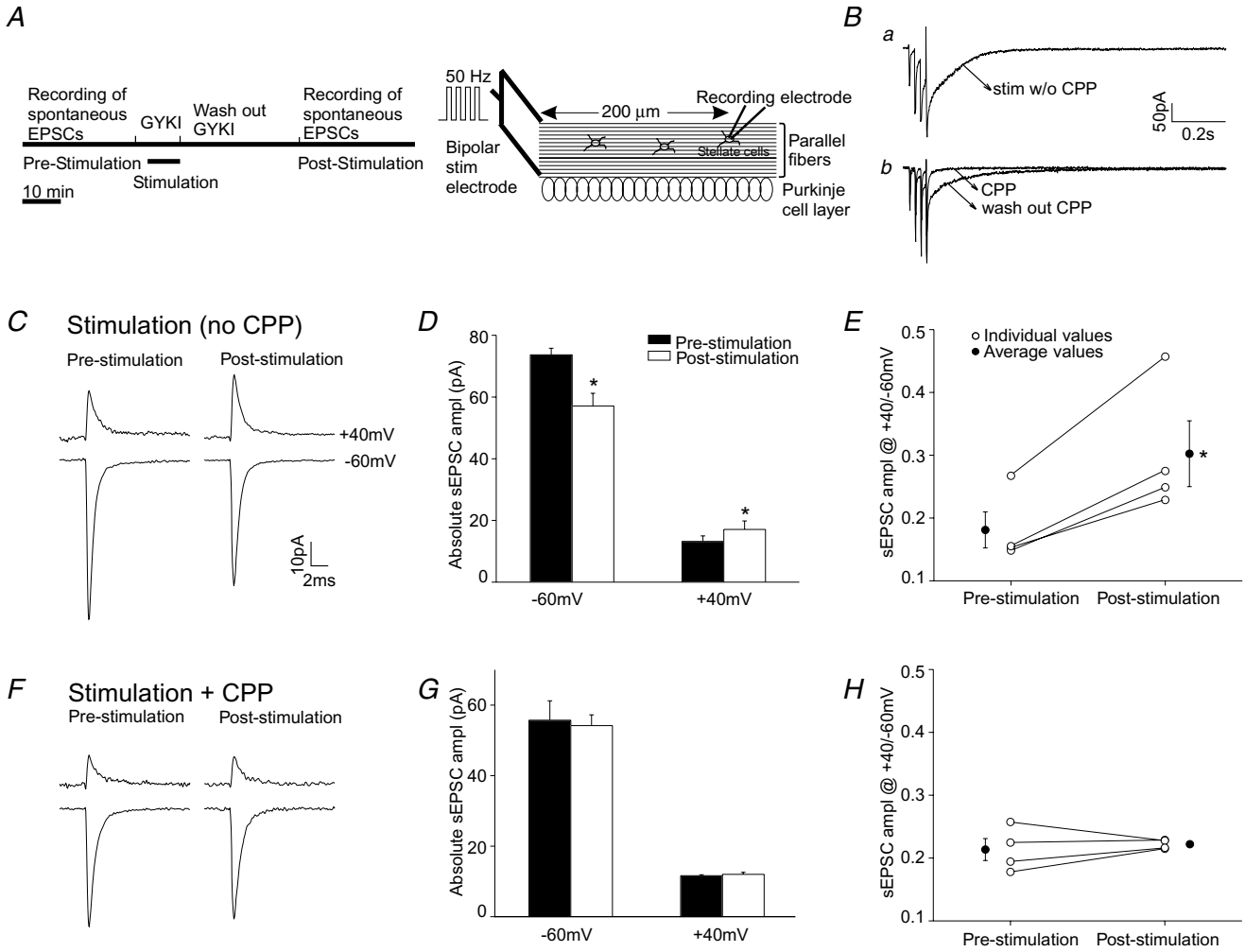

Figure 2. PF stimulation at 32°C induced a change in AMPAR subtypes in ACSF that contained 1 mM Mg
Spermine (100 µM) was included in the pipette solution. *A*, schematic of the experimental procedure. *Ba*, PF stimulation followed by a brief depolarization to 0 mV evoked an NMDAR current in ACSF that contained GYKI 52466 (upper trace). *Bb*, this stimulation protocol did not activate the current in the presence of CPP (lower trace). Stimulation intensity was above threshold. *C–E*, PF stimulation without CPP. *C*, average sEPSC current traces recorded at +40 mV and −60 mV before and 30 min after PF stimulation. *D*, group data of sEPSC amplitude ($n = 4$). *E*, ratio of sEPSC amplitude at +40 mV *versus* −60 mV of individual cells (○). Average values are shown as ●. *F–H*, parallel fibres were stimulated in the presence of 20 µM CPP to block NMDARs. *F*, sEPSC current traces. *G*, average sEPSC amplitude ($n = 4$). *H*, ratio of sEPSC amplitude at +40 mV *versus* −60 mV of individual cells (○) and average values (●). (*$P < 0.05$ paired *t* test.)

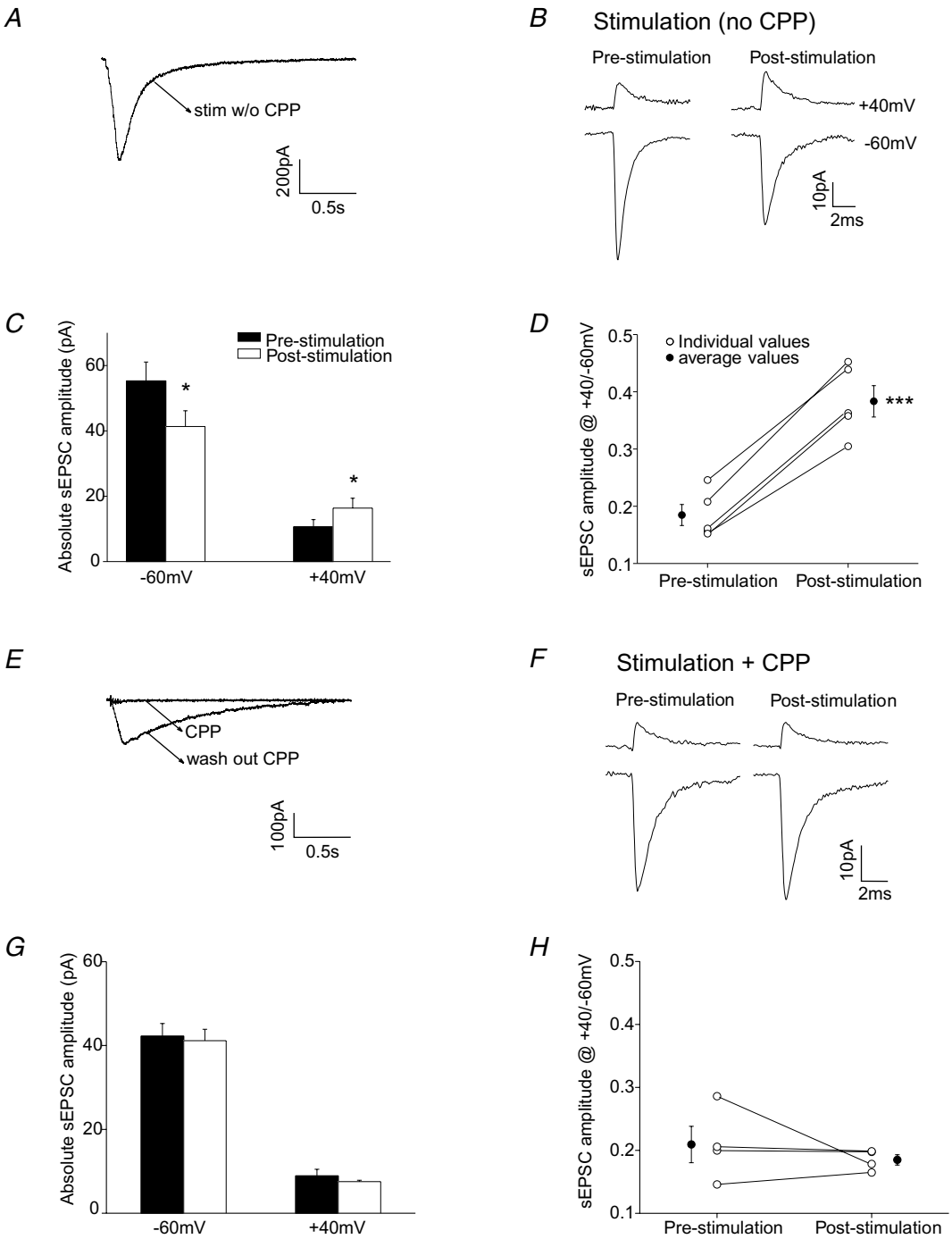

Figure 3. Activation of non-synaptic NMDARs by PF stimulation induced a change in the subunit composition of synaptic AMPARs

A, NMDAR currents evoked by PF stimulation (five depolarizations at 50 Hz) in the Mg^{2+}-free ACSF at room temperature. Stimulation intensity was above threshold. GYKI 52466 (50 μM) was present during the PF stimulation. *B*, average sEPSC current traces recorded at +40 mV and −60 mV before and 30 min after PF stimulation. *C*, group data of sEPSC amplitude ($n = 5$). *D*, ratio of sEPSC amplitude at +40 mV *versus* −60 mV of individual cells (○). Average values are shown as ●. *E–H*, parallel fibres were stimulated in the presence of 20 μM CPP to block NMDARs in the Mg^{2+}-free external solution. *E*, CPP blocked NMDAR currents evoked by PF stimulation. *F*, sEPSC current traces. *G*, average current amplitude ($n = 4$). *H*, ratio of sEPSC amplitude at +40 mV *versus* −60 mV of individual cells (○) and average values (●). (*$P < 0.05$; ***$P < 0.0005$.)

condition (Fig. 3*A*) suggests that this is comparable to the 'low-intensity' stimulation that elevates firing rate in stellate cells (Carter & Regehr, 2000). Intracellular spermine at 0.1 mM has little effect on NMDARs at negative potentials (Araneda *et al.* 1999; Turecek *et al.* 2004) and therefore is unlikely to significantly reduce NMDAR currents.

We then tested whether burst stimulation of PFs could induce a switch in AMPAR subtypes under physiological-like conditions (32°C in an external solution that contained 1 mM Mg^{2+}). Spontaneous EPSCs were recorded at +40 mV and −60 mV prior to and 30 min following PF stimulation. The ratio of sEPSC amplitude at +40 mV *versus* −60 mV was used to estimate the subunit composition of synaptic AMPARs. As illustrated in Fig. 2*C*, prior to the PF stimulation, sEPSCs displayed the characteristics of GluR2-lacking AMPARs, that is the current amplitude was reduced at depolarized potentials. PF stimulation evoked an inward current that was blocked by CPP, an NMDAR blocker (Fig. 2*B*). After the PF stimulation, the amplitude of sEPSCs decreased at −60 mV, but increased at +40 mV ($n = 4$; $P < 0.05$, paired *t* test; Fig. 2*C* and *D*). Since spermine blocks the current through GluR2-lacking receptors at depolarized potentials, the current at positive potentials was mediated by GluR2-containing receptors. Thus the potentiation of sEPSCs at +40 mV indicates that the number of GluR2-containing receptors increased. The decrease in sEPSC amplitude at −60 mV (via both GluR2-lacking and GluR2-containing receptors) indicates that a reduction in synaptic GluR2-lacking AMPARs had also occurred ($P < 0.05$). Consequently the ratio of the sEPSC amplitude at +40 mV *versus* − 60 mV increased following the PF stimulation from 0.18 ± 0.03 to 0.30 ± 0.05 ($P < 0.02$; Fig. 2*E*). This change occurred both at 32°C and at room temperature (supplemental Fig. 2). Thus some of the synaptic AMPARs had switched from GluR2-lacking receptors to GluR2-containing receptors.

We next determined whether the change in AMPAR subtypes was induced by activation of NMDARs. External solution containing 20 μM CPP (an NMDAR antagonist) and 50 μM GYKI 52466 was applied for 2 min prior to and during the burst stimulation of PFs. sEPSCs were recorded at +40 mV and −60 mV prior to and 30 min after PF stimulation. At the end of each experiment the parallel fibres were stimulated again in the presence of GYKI 52466 (without CPP), to make sure that the stimulation of the same parallel fibres could evoke a slow NMDAR current (Fig. 2*B*b).

As shown in Fig. 2*F* and *G*, burst stimulation of parallel fibre inputs in the presence of CPP failed to induce an increase in the sEPSC amplitude at +40 mV and a decrease at −60 mV. The ratio of sEPSC amplitude at +40 mV *versus* −60 mV also remained unaltered (Fig. 2*H*). Thus, activation of NMDARs induced a switch in AMPAR subtypes in stellate cells.

The activation of extrasynaptic NMDARs can be enhanced by reducing the extracellular Mg^{2+} concentration. Thus an increase in NMDAR activation would be expected to produce a larger change in AMPAR subtypes. This was found to be the case. When the experiment was performed in a Mg^{2+}-free solution at room temperature, PF stimulation evoked a large NMDAR-mediated current (Fig. 3*A* and supplemental Fig. 3). The sEPSC amplitude increased at +40 mV ($n = 5$, $P < 0.05$), but decreased at −60 mV ($P < 0.05$) following PF stimulation (Fig. 3*B* and *C*). As predicted, PF stimulation induced a more pronounced increase in the ratio of sEPSC amplitude (R) in the Mg^{2+}-free solution (from 0.18 ± 0.02 to 0.38 ± 0.03; $\Delta R = 0.20 \pm 0.02$; Fig. 3*D*) than at 32°C in the presence of 1 mM Mg^{2+} ($\Delta R = 0.12 \pm 0.02$; $P < 0.03$). Under the former conditions, the activity-induced changes were again blocked by CPP applied during the PF stimulation (Fig. 3*E*–*H*). These results support the idea that the repetitive activation of NMDARs caused by the spillover of glutamate released from parallel fibres during a train of presynaptic activity altered the subunit composition of synaptic AMPARs in stellate cells.

Activation of NMDA receptors induces a lasting change in AMPAR subtypes

To determine whether activation of NMDARs was sufficient to alter the subunit composition of AMPARs present at the synapse, NMDARs were directly activated by the exogenous application of NMDAR agonists, NMDA and glycine. Application of NMDA and glycine did not elevate mEPSC frequency. Since the synaptic current at the parallel fibre-to-stellate cell synapse is mediated solely by AMPARs (Clark & Cull-Candy, 2002), bath application of NMDA and glycine is expected to activate extrasynaptic NMDARs. NMDA application does not increase mEPSC frequency or evoke an increase in parallel fibre Ca^{2+} concentration (Glitsch & Marty, 1999; Shen & Linden, 2005). Following a control period during which sEPSCs were recorded, 20 μM NMDA plus 50 μM glycine were applied for 3 min in the Mg^{2+}-free extracellular solution, while the postsynaptic cell was voltage clamped at −30 mV. Under these conditions the sEPSC amplitude increased at +40 mV ($n = 5$, $P < 0.05$), and decreased at −60 mV ($n = 5$, $P < 0.02$; Fig. 4*A* and *H*) following the NMDA/glycine application. The increase in EPSC amplitude at +40 mV was not due to the recruitment of NMDARs into the postsynaptic site, because CPP did not reduce the sEPSC amplitude or decay time (sEPSC amplitude at +40 mV after NMDA application was 12.1 ± 1.0 pA and 13 ± 1.1 pA, and the decay time constants were 1.22 ± 0.09 ms and 1.37 ± 0.21 ms, in the

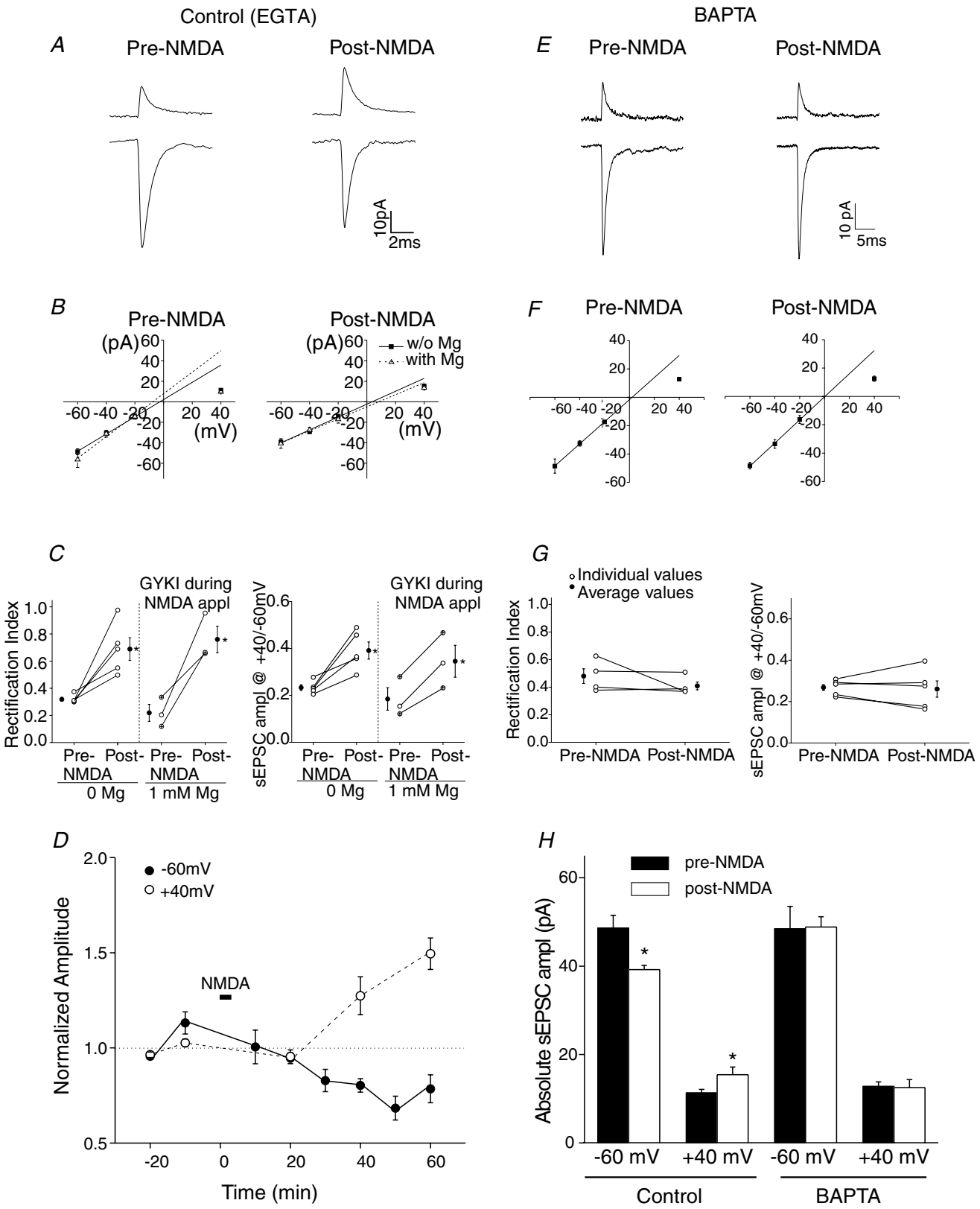

Figure 4. BAPTA blocked the NMDA-induced change in AMPAR subtypes
A brief application of NMDA induced a lasting change in synaptic AMPAR subtypes (*A–D*). This effect was blocked when 10 mM BAPTA was included in the patch electrode (*E–G*). Experiments were performed in a Mg^{2+}-free (*A–G*) or regular external (*B* and *C*) solution that contained 1 mM Mg^{2+} (50 μM GYKI was present during NMDA

absence and presence of CPP, respectively, $n = 5, P > 0.05$). The simultaneous increase in the sEPSC amplitude at +40 mV and reduction at −60 mV are consistent with the idea that the number of synaptic GluR2-containing receptors increased while GluR2-lacking receptors were lost following the application of NMDA.

The *I–V* relationship of the synaptic current changed from inwardly rectifying to nearly linear after application of NMDA (Fig. 4*B*), as reflected by an increase in the rectification index ($n = 5$, $P < 0.02$, Fig. 4*C*). The change in the *I–V* relation indicates that synaptic AMPARs switched from GluR2-lacking to GluR2-containing receptors. In agreement with the notion of an AMPAR subunit change, the ratio of current amplitudes at +40 mV *versus* −60 mV increased in all cells recorded ($P < 0.02$, Fig. 4*C*).

These changes were observed ∼30 min after NMDA application and lasted for at least a further 30 min, indicating that a sustained alteration in synaptic AMPAR subtypes had occurred (Fig. 4*D*). Without any stimulation, the sEPSC amplitude remained constant at −60 mV and +40 mV for at least 1 h ($n = 7$, supplemental Fig. 4*A*). Thus the potentiation of sEPSC amplitude at +40 mV and the suppression at −60 mV are triggered by NMDA application.

To test whether Ca^{2+} influx through NMDARs in postsynaptic stellate cells triggers the change in synaptic currents, BAPTA (10 mM) was included in the patch electrode to buffer any Ca^{2+} rise in the postsynaptic cell. Following NMDA application, the rectification index of the synaptic currents did not alter ($n = 5$, Fig. 4*E–H*). This result is consistent with the idea that activation of NMDARs in the postsynaptic cell induces the switch in AMPAR subtypes.

We next tested the possibility that an increased glutamate release from granule cells during the NMDA application may have activated Ca^{2+}-permeable AMPARs, thus altering the subunit composition of synaptic AMPARs. This experiment was carried out in the regular external solution that contained 1 mM $MgCl_2$. GYKI 52466 (50 μM) was applied 2 min before and during the application of NMDA and was then removed by continuous washout with ACSF for 30 min. Blocking AMPARs with GYKI 52466 during the NMDA application did not prevent the NMDA-induced increase in the rectification index of sEPSCs and the ratio of current amplitudes at +40 mV *versus* −60 mV ($n = 3$; $P < 0.05$, Fig. 4*B–C*). Thus the activation of extrasynaptic NMDARs is sufficient to induce the exchange of synaptic AMPAR subtypes in cerebellar stellate cells.

Inhibition of PKC blocks the activity-dependent switch in AMPAR subtypes

We first determined whether PKC activity was involved in the constitutive recycling of synaptic AMPARs. Recording of sEPSCs started immediately after break-in, and sEPSCs were monitored for 1 h without any presynaptic stimulation. The amplitude of sEPSCs at −60 mV and +40 mV remained unchanged ($n = 7$, supplemental Fig. 4*A*). When 10 μM chelerythrine, a PKC inhibitor, was included in the pipette solution, the amplitude of sEPSCs at both +40 mV and −60 mV were unaltered ($n = 5$, supplemental Fig. 4*B*). We also used a structurally different PKC inhibitor, PKCI 19–36 (which acts as psudosubstrate by binding to the active site of PKC), and found that there was no change in the amplitude of sEPSCs at +40 mV or −60 mV ($n = 4$, supplemental Fig. 4*C*).

We next tested whether the activity-induced change in AMPAR subtypes necessarily requires the activation of PKC. For these experiments we examined whether infusion of PKC inhibitors into the stellate cell blocked the NMDA-induced increase in sEPSC amplitude at +40 mV. As shown in Fig. 5*A–C*, application of NMDA did not alter the current amplitude at +40 mV when PKCI 19–36 (20 μM) was present. Thus PKCI 19–36 prevented the increase in the sEPSC amplitude at +40 mV, suggesting that the NMDAR-dependent delivery of GluR2-containing receptors requires the activation of PKC.

Although the activation of NMDARs induced a decrease in sEPSC amplitude at −60 mV (Figs 2–4), it failed to alter the current amplitude at −60 mV in the presence of PKCI 19-36 (Fig. 5*A–C*). This result indicates that the activity-induced loss of GluR2-lacking receptors is

application). *A*, average current traces at +40 mV and −60 mV prior to and 30 min following the application of 20 μM NMDA and 50 μM glycine. *B*, *I–V* relationship of sEPSCs prior to and following NMDA application. *C* left, rectification index determined from the *I–V* relationship of individual cells (○). The average rectification index (●) increased. Right, ratio of sEPSC amplitude at +40 mV *versus* −60 mV from individual cells (○: pipette solution containing 0.5 mM EGTA; open circles with a cross: 10 mM EGTA pipette solution). Average values increased (●; $^*P < 0.05$). *D*, sEPSC amplitude was normalized to that prior to NMDA application at each potential. *E–G*, sEPSCs were recorded using a pipette solution that contained 10 mM BAPTA. *E*, BAPTA blocked the NMDA-induced change in sEPSC amplitude. *F*, NMDA application failed to induce a change in the *I–V* relationship of sEPSCs ($n = 5$). *G*, rectification index and ratio of sEPSC amplitude at +40 mV *versus* −60 mV remained unaltered following NMDA application. *H*, average sEPSC amplitude increased at +40 mV and declined at −60 mV ($n = 5$) using the control pipette solution; the current amplitude did not change when using a BAPTA-containing pipette solution.

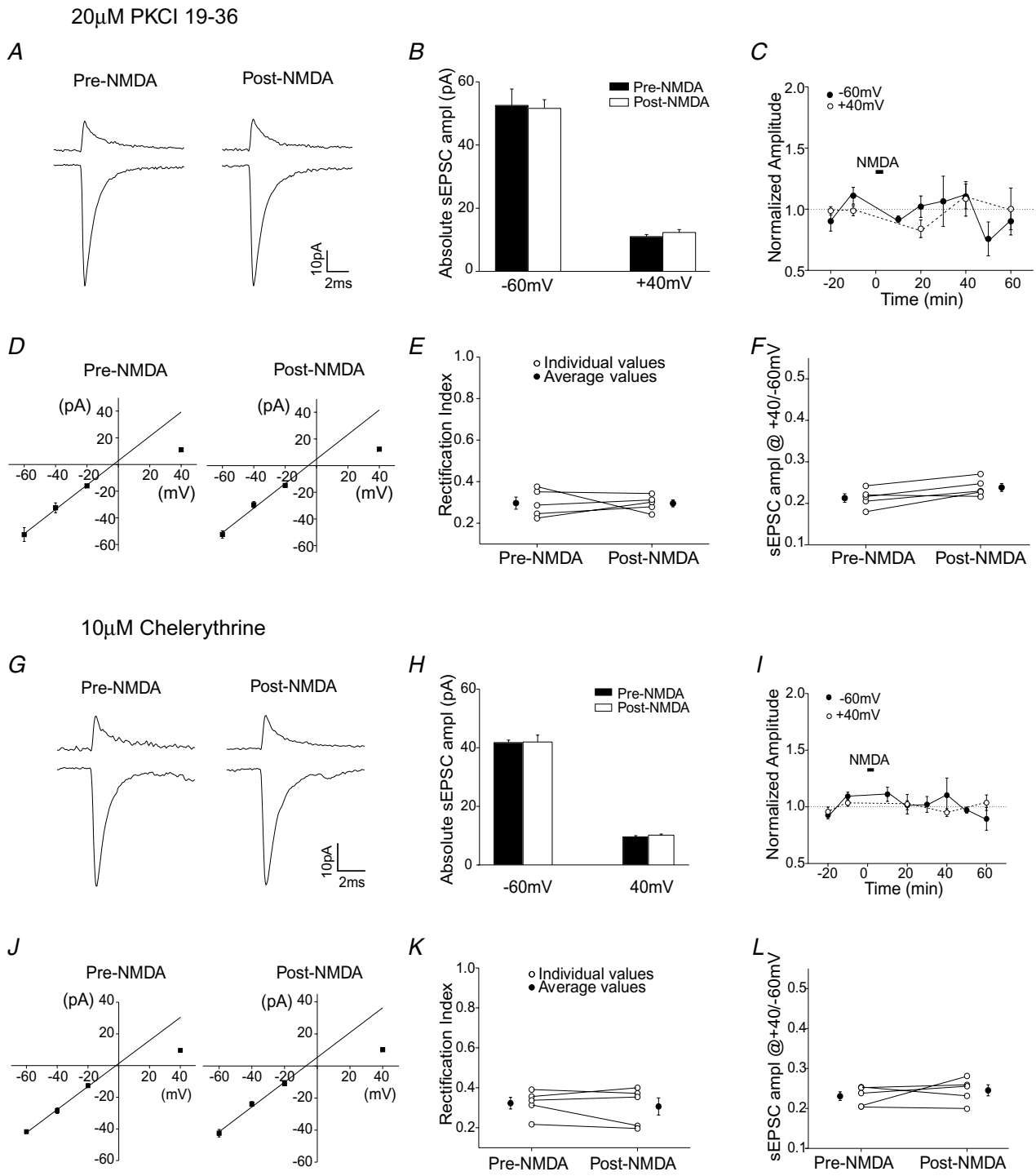

Figure 5. Intracellular application of KCl 19-36 and chelerythrine blocked the NMDA-induced switch in AMPAR subtypes

A–F, PKCI 19-36 (20 μM) was included in the pipette solution. A, examples of average sEPSC traces at +40 mV and −60 mV. *B*, group data of sEPSC amplitude ($n = 5$). *C*, sEPSC amplitude normalized to that prior to NMDA application at each potential *versus* time. *D*, *I–V* relationship of synaptic currents. E, rectification index of individual cells (○) and the average value (●). *F*, ratio of sEPSC amplitude at +40 mV *versus* −60 mV of individual cells (○) and average values (●). *G–L*, chelerythrine (10 μM) was added to the pipette solution. *G*, average sEPSCa at +40 mV and −60 mV before and after the application of NMDA. *H*, group data of sEPSC amplitude at these potentials ($n = 5$). *I*, sEPSC amplitude normalized to that prior to NMDA application at each potentials *versus* time. *J*, *I–V* relationship of sEPSCs prior to and following the application of NMDA. *K*, rectification index of individual cells (○) and average value (●). *L*, ratio of sEPSC amplitude at +40 mV *versus* −60 mV of individual cells (○) and average values (●).

also prevented. Thus PKC activation appears to be involved both in the insertion of Ca^{2+}-impermeable AMPARs and in the removal of Ca^{2+}-permeable AMPARs. However another possibility is that these two processes are coupled.

Consistent with these observations, PKCI 19-36 also blocked the NMDA-induced change in the *I–V* relationship of sEPSCs, which remained inwardly rectifying after the application of NMDA (Fig. 5*D* and *E*). The ratio of sEPSC amplitude at +40 mV *versus* −60 mV did not change (Fig. 5*F*). Thus, the activity-dependent switch in AMPAR subtypes was prevented by this PKC peptide inhibitor.

To ensure that the effect of PKCI 19-36 was due to the inhibition of PKC activity, we also tested another PKC inhibitor, chelerythrine. Chelerythrine (10 μM) prevented the NMDA-induced change in the amplitude of sEPSCs at +40 mV and −60 mV (Fig. 5*G–I*). The rectification index of the *I–V* relationship and the ratio of sEPSC amplitude at +40 mV *versus* −60 mV remained unaltered (Fig. 5*J–L*). Therefore chelerythrine also blocked the NMDA-induced switch in AMPAR subtypes. These results strongly suggest that activation of PKC is required for the NMDA-induced increase in GluR2-containing and loss of GluR2-lacking receptors.

Activation of PKC increases synaptic GluR2-containing AMPARs

Is activation of PKC sufficient to trigger the change in AMPAR subtypes at the synapse? To address this question, we included a PKC activator (−)indolactam-V, in the pipette solution (Shen & Linden, 2005). In a separate set of experiments, the inactive isomer (+)indolactam-V, or vehicle (DMSO) was used as a control. sEPSCs at various holding potentials were measured 15 min after obtaining the whole-cell configuration.

In the control experiments, the synaptic current had an inwardly rectifying *I–V* relationship, as found in the presence of 300 μM (+)indolactam-V or DMSO. The rectification index was 0.27 ± 0.01 ($n = 7$) for (+)indolactam-V and 0.27 ± 0.04 ($n = 4$) for the DMSO control. However the rectification index increased to 0.64 ± 0.13 ($n = 7$) when 300 μM (−)indolactam-V was present ($P < 0.05$; (−)indolactam-V *versus* (+)indolactam-V), indicating that the synaptic receptors were less permeable to Ca^{2+} when PKC was activated (Fig. 6*A*, *B* and *D*).

The amplitude of synaptic currents at +40 mV changed from 9.6 ± 0.6 pA in (+)indolactam-V control to 12.2 ± 0.8 pA in the presence of (−)indolactam-V ($n = 7$; $P < 0.02$). This 27% increase in the EPSC amplitude is comparable to the increase at +40 mV that followed PF stimulation and NMDA application (Figs 2–4). The potentiation of synaptic current at +40 mV is consistent with the idea that activation of PKC increases the expression of GluR2-containing receptors at the synapse.

Activation of NMDARs also induced a decrease in the synaptic current at −60 mV, which was blocked by PKC inhibitors (Figs 2–5). However in the presence of (−)indolactam-V, the EPSC amplitude at −60 mV was not reduced compared with (+)indolactam-V ($P = 0.17$; $n = 7$). If the number of GluR2-lacking receptors remained constant at the synapse, one would expect to see an enhancement of the EPSC amplitude at −60 mV due to the increase in GluR2-containing receptors. Since activation of PKC by (−)indolactam-V potentiates the current amplitude at +40 mV by 3 pA, the current at −60 mV should increase by 4.5 pA. There is an apparent, but not significant, increase in the amplitude of synaptic currents at −60 mV (from -54.4 ± 3.3 pA to -60.3 ± 2.5 pA), which may account for the elevated level of GluR2-containing receptors at the synapse. These data are consistent with the idea that PKC activation causes an increase in the GluR2-containing receptors and has little effect on the GluR2-lacking receptors at the synapse.

In further support of a PKC-dependent increase in GluR2-containing receptors, infusion of another PKC activator, OAG (1-oleoyl-2-acetyl-sn-glycerol 20 μM), into stellate cells also enhanced the sEPSC amplitude at +40 mV ($P < 0.005$) but did not change the synaptic current at −60 mV ($P = 0.33$), compared to the DMSO control. The synaptic current displayed a linear *I–V* relationship (Fig. 6*C* and *D*), with a rectification index of 0.89 ± 0.02. Thus activation of PKC is necessary and sufficient to cause the delivery of GluR2-containing receptors, so increasing the levels of GluR2-containing AMPARs at the synapse. PKC activation is necessary but not sufficient to trigger the activity-induced loss of GluR2-lacking receptors.

PICK is involved in the NMDA-induced increase in GluR2-containing receptors

Activated PKC is known to interact with PICK, which binds to GluR2 subunits and facilitates targeting of GluR2 to synapses (Perez *et al.* 2001). Our previous study showed that disrupting the PICK–GluR2 interaction blocked the activity-dependent increase in GluR2 expression at the synapse (Liu & Cull-Candy, 2005). We therefore determined whether the PICK–GluR2/3 interaction is also required for the NMDAR-induced delivery of GluR2-containing AMPARs.

A peptide inhibitor, pep2-AVKI (NVYGIEAVKI; 0.5 mM), was included in the pipette solution to selectively block the interaction between PICK and GluR2/3 (Osten *et al.* 2000). This peptide does not affect basal transmission at the parallel fibre-to-stellate cell synapse (Liu & Cull-Candy, 2005). sEPSCs were measured at various potentials prior to and following NMDA

application. As shown in Fig. 7, when the postsynaptic cell contained pep2-AVKI, activation of NMDARs now failed to increase the sEPSC amplitude at +40 mV. Thus pep2-AVKI prevented the NMDAR-induced increase in the sEPSC amplitude at positive potentials (Fig. 7*A–C*) that is mediated entirely by GluR2-containing receptors. In contrast, the sEPSC amplitude at −60 mV decreased ($n = 5$; $P < 0.05$) following NMDA application.

To test whether the inhibitory effect of pep2-AVKI on the NMDA-induced change was due to its selective binding to PICK, we examined the effects of an inactive control peptide (NVYGIESVKE, pep2-SVKE) that does not bind to PICK. As expected, NMDA application now produced an increase in sEPSC amplitude at +40 mV ($n = 6$; $P < 0.05$), and a decrease at −60 mV ($P < 0.05$; Fig. 7*D–F*). Thus the disruption of the GluR2–PICK interaction by the binding of pep2-AVKI to PICK prevented the activity-dependent increase in GluR2-containing receptors.

These results support the view that both the interaction between GluR2 and PICK and the activation of PKC are required for the NMDAR-dependent delivery of AMPARs containing GluR2 to these synapses.

Discussion

Our results suggest that the activity of extrasynaptic NMDARs can control the dynamic movement of AMPARs at the synapse *via* intracellular signalling pathways. We have shown that the physiological-like activation of extrasynaptic NMDARs can produce a long-lasting change in the subunit composition of synaptic AMPARs. This switch involved an increase in GluR2-containing receptors and a decrease in GluR2-lacking receptors at the synapse. PICK and PKC activity drive the delivery of GluR2-containing receptors. PKC activation is necessary but not sufficient for the loss of GluR2-lacking receptors.

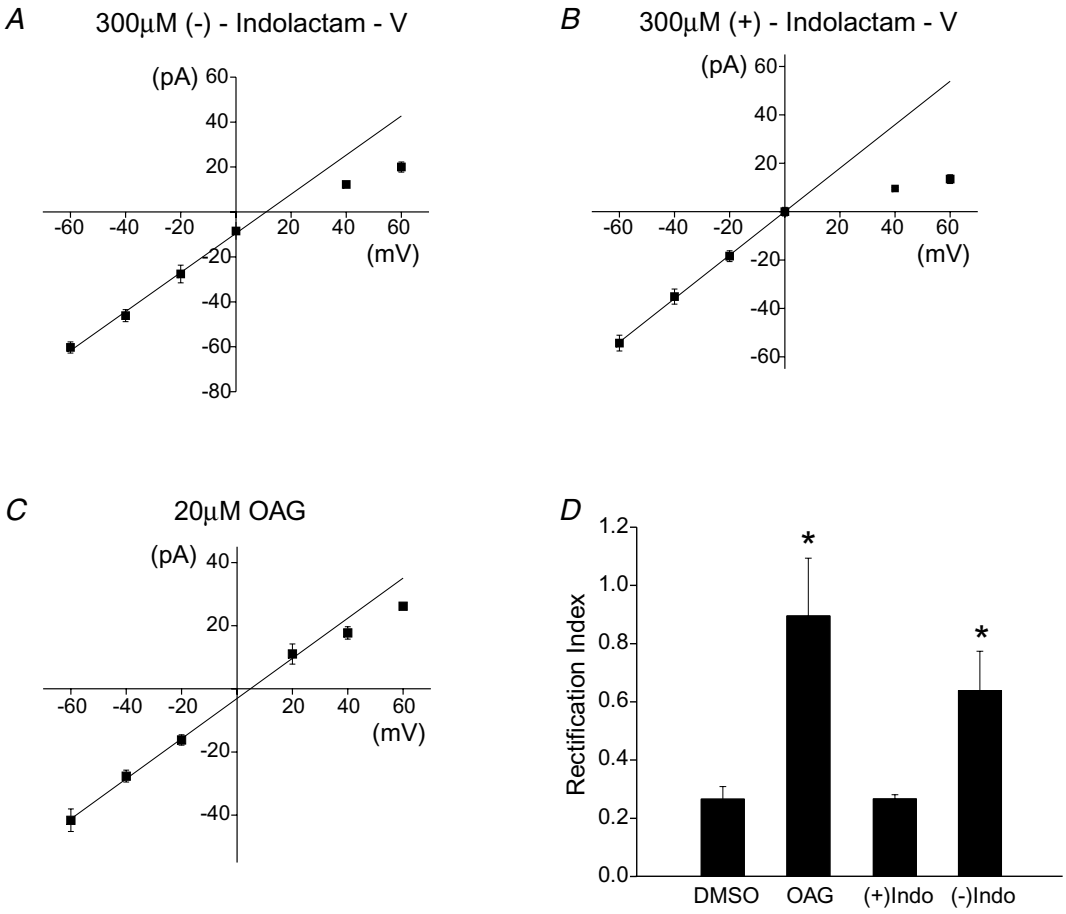

Figure 6. Activation of PKC by (−)indolactam-V or OAG changed the subunit composition of the AMPARs at the synapse
A, *I–V* relationship of sEPSCs when (−)indolactam-V (300 μM) was included in the pipette solution ($n = 7$). *B*, (+)indolactam-V was used as a negative control ($n = 7$). *C*, inclusion of OAG in the patch electrode gave rise to a linear *I–V* relationship of sEPSCs ($n = 5$). *D*, rectification index of synaptic currents increased in the presence of (−)indolactam-V and OAG (DMSO control, $n = 4$; $^*P < 0.05$).

NMDARs are present at many excitatory synapses as well as in extrasynaptic regions (Tovar & Westbrook, 2002; Scimemi *et al.* 2004). In some cells they are localized exclusively at extrasynaptic sites (Chen & Diamond, 2002; Clark & Cull-Candy, 2002). Unlike synaptic NMDARs that can be activated by a single quantum of transmitter, glutamate spillover contributes to the activation of extrasynaptic NMDARs (Carter & Regehr, 2000; Diamond,

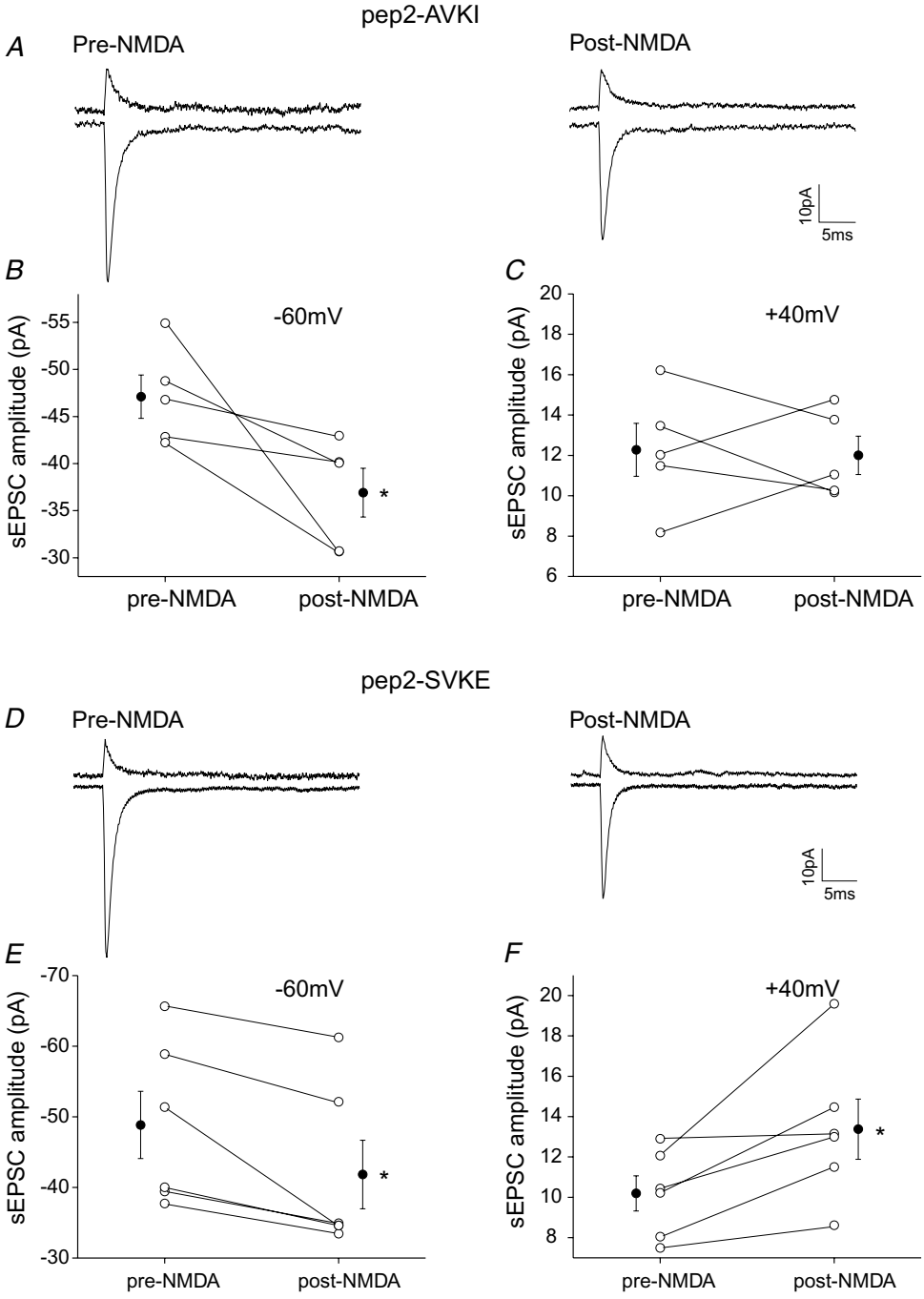

Figure 7. pep2-AVKI blocked the NMDAR-induced increase in sEPSC amplitude at +40 mV
A–C, pep2 AVKI (0.5 mM) or *D–F*, a control peptide pep2SVKE was included in the pipette solution. *A* and *D*, averaged spontaneous EPSCs at +40 mV and −60 mV, prior to and following NMDA application. *B* and *E*, comparison of sEPSC amplitude in individual cells (○) and average value (●) at −60 mV before and after NMDA application. *C* and *F*, comparison of sEPSC amplitude in individual cells (○) and average value (●) at +40 mV before and after NMDA application. Note that the NMDA application induced an increase in the sEPSC amplitude at +40 mV and a decrease at −60 mV when the control peptide was included. The increase in sEPSC amplitude at +40 mV was blocked when pep2-AVKI was present. (*$P < 0.05$; pep2-AVKI: $n = 5$; pep2-SVKI: $n = 6$.)

2001). The proposed functions of extrasynaptic NMDARs involve cooperative interactions between neighbouring hippocampal synapses (Arnth-Jensen *et al.* 2002) and regulation of cAMP response element-binding protein (CREB) activity which is coupled to cell death pathways (Hardingham *et al.* 2002). Our results reveal another role for extrasynaptic NMDARs – namely the induction of a long-term change in synaptic AMPARs.

Glutamate spillover can be evoked by high-frequency stimulation of presynaptic terminals and is controlled by glutamate uptake into neurons and glia by excitatory amino acid transporters (Fellin *et al.* 2004; Huang & Bergles, 2004). Our experiments suggest that a burst of PF activity that mimics the behaviour of granule cells evoked by sensory stimulation can alter synaptic AMPAR subtypes by activating extrasynaptic NMDARs. One prediction of this work is that glutamate spillover that is caused by a reduction of glutamate transporter activity may also induce a long-term change in synaptic AMPARs by activating extrasynaptic NMDARs. Indeed pharmacological blockade of glutamate uptake can activate extrasynaptic NMDARs in cortical neurons, thereby leading to the induction of LTD (Massey *et al.* 2004). Conversely reducing glutamate transporter activity by lowering the temperature allows the glutamate that is released from the stimulated synapses to activate NMDARs and induces LTP at unstimulated synapses in the amygdala (Tsvetkov *et al.* 2004). There is evidence that presynaptic stimulation can also alter glutamate transporter currents in Purkinje and pyramidal cells, presumably by regulating their transport function or trafficking (Davis *et al.* 1998; Lin *et al.* 2001; Levenson *et al.* 2002; Fournier *et al.* 2004; Shen & Linden, 2005).

Although activation of extrasynaptic NMDARs or postsynaptic AMPARs can induce similar changes in postsynaptic AMPAR subtypes, there are distinct differences in the induction mechanisms. First, synaptic AMPARs can be activated by spontaneous basal activity as well as by the high-frequency PF stimulation, thus producing an increase in GluR2-containing subtypes at the synapse (Liu & Cull-Candy, 2000, 2002). In contrast, extrasynaptic NMDARs can only be activated by a burst of high-frequency presynaptic stimulation (Carter & Regehr, 2000). Therefore extrasynaptic NMDARs may serve as a 'sensor' that detects the pattern of presynaptic activity and, once activated, gates synaptic plasticity. Second, repetitive activation of synaptic AMPARs induces a change in AMPAR subtypes at the same synapse, and therefore is a form of homosynaptic plasticity. Our results indicate that Ca^{2+} entry *via* extrasynaptic NMDARs is sufficient to modulate synaptic AMPARs that are located some distance away. Since NMDARs are located outside of the synapse, the change they induce may not necessarily be input specific. This raises the possibility that the Ca^{2+} entry *via* extrasynaptic NMDARs that is induced by the stimulation of one afferent pathway could potentially alter the AMPAR subtypes not only at the same synapse but also at nearby synapses that are not activated by the presynaptic stimulus. This would lead to a homosynaptic and possibly heterosynaptic switch in AMPAR subtypes.

The changes in synaptic AMPAR currents following the activation of extrasynaptic NMDARs share the same features as those induced by Ca^{2+} entry *via* Ca^{2+}-permeable AMPARs (Liu & Cull-Candy, 2000, 2005). First, activation of extrasynaptic NMDARs results in a 36% increase in the sEPSC amplitude at +40 mV and a 20% decrease at −60 mV. This leads to a two-fold increase in the rectification index of sEPSCs. Second, we have previously reported that the average conductance of Ca^{2+}-impermeable receptors (∼5.5 pS) is about 23% lower than that of AMPARs that display partial inward rectification in stellate cells (∼7.2 pS) (Liu & Cull-Candy, 2005). Thus the reduction in channel conductance can account for the change in sEPSC amplitude associated with the NMDAR-induced switch in AMPAR subtypes. This suggests that some of the GluR2-lacking receptors that left the synapse were replaced by GluR2-containing receptors. Third, intracellular BAPTA (but not EGTA) blocked the NMDAR-induced change in the *I–V* relationship. Since BAPTA binds to Ca^{2+} more rapidly than does EGTA, the extrasynaptic NMDARs may be located closer to the synaptic regions (Adler *et al.* 1991). Thus Ca^{2+} entry *via* extrasynaptic NMDARs triggers the targeting of GluR2s. In turn this leads to a reduction in Ca^{2+} influx through synaptic AMPARs, and this provides a negative feedback mechanism. These observations suggest that the switch in synaptic AMPAR subtypes that is induced by activating two different glutamate receptors may share a similar molecular mechanism.

Our results show that PKC activation and PICK are required for the NMDAR-induced increase in GluR2-containing receptors at the synapse. This is consistent with recent studies that revealed that PICK and the N-ethylmaleimide sensitive fusion protein (NSF) drive the activity-dependent delivery of GluR2-containing receptors to the PF–stellate cell synapse (Gardner *et al.* 2005; Liu & Cull-Candy, 2005). PICK is known to interact with activated PKC, and activation of PKC induces redistribution of PICK–GluR2 complexes to spines in hippocampal neurons (Staudinger *et al.* 1995; Dev *et al.* 1999; Perez *et al.* 2001). These results support the notion that Ca^{2+} entry via extrasynaptic NMDARs activates PKC, which could bind to PICK and drive the insertion of GluR2-containing receptors to the synapse. In keeping with this idea both PICK and PKC are required for 5-HT-induced LTP in dorsal horn neurons (Li *et al.* 1999). However, this model contrasts with work in hippocampal and Purkinje cells, in which the loss of GluR2-containing receptors during LTD requires PICK and PKC (Daw *et al.* 2000; Xia *et al.* 2000; Kim *et al.* 2001; Leitges *et al.* 2004).

Our experiments showed that inhibition of PKC also blocked the NMDA-induced reduction of

sEPSCs at −60 mV, and thus prevented the loss of GluR2-lacking receptors that requires disruption of the AMPAR–GRIP interaction (Liu & Cull-Candy, 2005). Because phosphorylation of GluR2 by PKC can disrupt the GRIP–GluR2 interaction (Matsuda *et al.* 1999; Chung *et al.* 2000), activation of PKC may also interfere with the interaction between GluR2-lacking receptors and GRIP via a similar mechanism. GRIP is known to bind to the C-terminus of GluR2/3/4c subunits (Dong *et al.* 1997; Srivastava *et al.* 1998; Dong *et al.* 1999). Stellate cells appear to express all three subunits (Keinanen *et al.* 1990; Sato *et al.* 1993; Petralia *et al.* 1997; Gardner *et al.* 2005), and hence GluR2-lacking receptors are likely to contain GluR3/4 subunits. Given that the PKC phosphorylation site at the C-terminal of the GluR3 subunit is conserved (Song & Huganir, 2002), this suggests that PKC might cause phosphorylation of GluR3 subunits. However the PKC activators (−)indolactam-V and OAG, did not reduce the current amplitude at −60 mV, indicating that the activity-dependent loss of GluR2-lacking receptors may require both PKC activation and other signalling molecules.

While our results are consistent with the PKC-mediated regulation of AMPAR trafficking in stellate cells, phosphorylation of AMPARs can also alter channel properties and modify synaptic transmission. Direct phophorylation of Ser831 on GluR1 by CaMKII and PKC causes an increase in the channel conductance and contributes to hippocampal LTP (Benke *et al.* 1998; Derkach *et al.* 1999; Lee *et al.* 2003). LTD on the other hand is associated with dephosphorylation of Ser 845 on GluR1 by PKA, which reduces the open channel probability (Banke *et al.* 2000; Lee *et al.* 2000). If the single-channel properties of synaptic AMPARs were altered due to phosphorylation of AMPARs in stellate cells, one would expect to see an increase in the sEPSC amplitude at both hyperpolarized and depolarized potentials. However, we observed an increase in current amplitude at +40 mV but a decrease at −60 mV. This result is best explained by a change in AMPAR subtypes.

In conclusion, our results suggest that the trafficking of synaptic AMPAR subtypes is controlled by the activity of extrasynaptic NMDARs. These receptors are sensitive to the pattern of presynaptic activity because they are only activated by stimulus trains that cause glutamate spillover. It will be of interest to determine whether the PKC activation that is triggered by activation of extrasynaptic NMDARs induces a localized or global change in synaptic AMPAR subtypes.

References

Adler EM, Augustine GJ, Duffy SN & Charlton MP (1991). Alien intracellular calcium chelators attenuate neurotransmitter release at the squid giant synapse. *J Neurosci* **11**, 1496–1507.

Akazawa C, Shigemoto R, Bessho Y, Nakanishi S & Mizuno N (1994). Differential expression of five *N*-methyl-D-aspartate receptor subunit mRNAs in the cerebellum of developing and adult rats. *J Comp Neurol* **347**, 150–160.

Araneda RC, Lan JY, Zheng X, Zukin RS & Bennett MV (1999). Spermine and arcaine block and permeate *N*-methyl-D-aspartate receptor channels. *Biophys J* **76**, 2899–2911.

Arnth-Jensen N, Jabaudon D & Scanziani M (2002). Cooperation between independent hippocampal synapses is controlled by glutamate uptake. *Nat Neurosci* **5**, 325–331.

Bagal AA, Kao JP, Tang CM & Thompson SM (2005). Long-term potentiation of exogenous glutamate responses at single dendritic spines. *Proc Natl Acad Sci U S A* **102**, 14434–14439.

Banke TG, Bowie D, Lee H, Huganir RL, Schousboe A & Traynelis SF (2000). Control of GluR1 AMPA receptor function by cAMP-dependent protein kinase. *J Neurosci* **20**, 89–102.

Benke TA, Luthi A, Isaac JT & Collingridge GL (1998). Modulation of AMPA receptor unitary conductance by synaptic activity. *Nature* **393**, 793–797.

Bowie D & Mayer ML (1995). Inward rectification of both AMPA and kainate subtype glutamate receptors generated by polyamine-mediated ion channel block. *Neuron* **15**, 453–462.

Bredt DS & Nicoll RA (2003). AMPA receptor trafficking at excitatory synapses. *Neuron* **40**, 361–379.

Carter AG & Regehr WG (2000). Prolonged synaptic currents and glutamate spillover at the parallel fiber to stellate cell synapse. *J Neurosci* **20**, 4423–4434.

Chadderton P, Margrie TW & Hausser M (2004). Integration of quanta in cerebellar granule cells during sensory processing. *Nature* **428**, 856–860.

Chen S & Diamond JS (2002). Synaptically released glutamate activates extrasynaptic NMDA receptors on cells in the ganglion cell layer of rat retina. *J Neurosci* **22**, 2165–2173.

Chung HJ, Steinberg JP, Huganir RL & Linden DJ (2003). Requirement of AMPA receptor GluR2 phosphorylation for cerebellar long-term depression. *Science* **300**, 1751–1755.

Chung HJ, Xia J, Scannevin RH, Zhang X & Huganir RL (2000). Phosphorylation of the AMPA receptor subunit GluR2 differentially regulates its interaction with PDZ domain-containing proteins. *J Neurosci* **20**, 7258–7267.

Clark BA & Cull-Candy SG (2002). Activity-dependent recruitment of extrasynaptic NMDA receptor activation at an AMPA receptor-only synapse. *J Neurosci* **22**, 4428–4436.

Davis KE, Straff DJ, Weinstein EA, Bannerman PG, Correale DM, Rothstein JD & Robinson MB (1998). Multiple signaling pathways regulate cell surface expression and activity of the excitatory amino acid carrier 1 subtype of Glu transporter in C6 glioma. *J Neurosci* **18**, 2475–2485.

Daw MI, Chittajallu R, Bortolotto ZA, Dev KK, Duprat F, Henley JM, Collingridge GL & Isaac JT (2000). PDZ proteins interacting with C-terminal GluR2/3 are involved in a PKC-dependent regulation of AMPA receptors at hippocampal synapses. *Neuron* **28**, 873–886.

Derkach V, Barria A & Soderling TR (1999). Ca^{2+}/calmodulin-kinase II enhances channel conductance of alpha-amino-3-hydroxy-5-methyl-4-isoxazolepropionate type glutamate receptors. *Proc Natl Acad Sci U S A* **96**, 3269–3274.

Dev KK, Nishimune A, Henley JM & Nakanishi S (1999). The protein kinase C alpha binding protein PICK1 interacts with short but not long form alternative splice variants of AMPA receptor subunits. *Neuropharmacology* **38**, 635–644.

Diamond JS (2001). Neuronal glutamate transporters limit activation of NMDA receptors by neurotransmitter spillover on CA1 pyramidal cells. *J Neurosci* **21**, 8328–8338.

Dong H, O'Brien RJ, Fung ET, Lanahan AA, Worley PF & Huganir RL (1997). GRIP: a synaptic PDZ domain-containing protein that interacts with AMPA receptors. *Nature* **386**, 279–284.

Dong H, Zhang P, Song I, Petralia RS, Liao D & Huganir RL (1999). Characterization of the glutamate receptor-interacting proteins GRIP1 and GRIP2. *J Neurosci* **19**, 6930–6941.

Fellin T, Pascual O, Gobbo S, Pozzan T, Haydon PG & Carmignoto G (2004). Neuronal synchrony mediated by astrocytic glutamate through activation of extrasynaptic NMDA receptors. *Neuron* **43**, 729–743.

Fournier KM, Gonzalez MI & Robinson MB (2004). Rapid trafficking of the neuronal glutamate transporter, EAAC1: evidence for distinct trafficking pathways differentially regulated by protein kinase C and platelet-derived growth factor. *J Biol Chem* **279**, 34505–34513.

Gardner SM, Takamiya K, Xia J, Suh JG, Johnson R, YuS & Huganir RL (2005). Calcium-permeable AMPA receptor plasticity is mediated by subunit–specific interactions with PICK1 and NSF. *Neuron* **45**, 903–915.

Glitsch M & Marty A (1999). Presynaptic effects of NMDA in cerebellar Purkinje cells and interneurons. *J Neurosci* **19**, 511–519.

Hardingham GE, Fukunaga Y & Bading H (2002). Extrasynaptic NMDARs oppose synaptic NMDARs by triggering CREB shut-off and cell death pathways. *Nat Neurosci* **5**, 405–414.

Huang YH & Bergles DE (2004). Glutamate transporters bring competition to the synapse. *Curr Opin Neurobiol* **14**, 346–352.

Kamboj SK, Swanson GT & Cull-Candy SG (1995). Intracellular spermine confers rectification on rat calcium-permeable AMPA and kainate receptors. *J Physiol* **486**, 297–303.

Keinanen K, Wisden W, Sommer B, Werner P, Herb A, Verdoorn TA, Sakmann B & Seeburg PH (1990). A family of AMPA-selective glutamate receptors. *Science* **249**, 556–560.

Kim CH, Chung HJ, Lee HK & Huganir RL (2001). Interaction of the AMPA receptor subunit GluR2/3 with PDZ domains regulates hippocampal long-term depression. *Proc Natl Acad Sci U S A* **98**, 11725–11730.

Koh DS, Burnashev N & Jonas P (1995). Block of native Ca^{2+}-permeable AMPA receptors in rat brain by intracellular polyamines generates double rectification. *J Physiol* **486**, 305–312.

Lee HK, Barbarosie M, Kameyama K, Bear MF & Huganir RL (2000). Regulation of distinct AMPA receptor phosphorylation sites during bidirectional synaptic plasticity. *Nature* **405**, 955–959.

Lee HK, Takamiya K, Han JS, Man H, Kim CH, Rumbaugh GYuS, Ding L, He C, Petralia RS, Wenthold RJ, Gallagher M & Huganir RL (2003). Phosphorylation of the AMPA receptor GluR1 subunit is required for synaptic plasticity and retention of spatial memory. *Cell* **112**, 631–643.

Leitges M, Kovac J, Plomann M & Linden DJ (2004). A unique PDZ ligand in PKCalpha confers induction of cerebellar long-term synaptic depression. *Neuron* **44**, 585–594.

Levenson J, Weeber E, Selcher JC, Kategaya LS, Sweatt JD & Eskin A (2002). Long-term potentiation and contextual fear conditioning increase neuronal glutamate uptake. *Nat Neurosci* **5**, 155–161.

Li P, Kerchner GA, Sala C, Wei F, Huettner JE, Sheng M & Zhuo M (1999). AMPA receptor–PDZ interactions in facilitation of spinal sensory synapses. *Nat Neurosci* **2**, 972–977.

Lin CI, Orlov I, Ruggiero AM, Dykes-Hoberg M, Lee A, Jackson M & Rothstein JD (2001). Modulation of the neuronal glutamate transporter EAAC1 by the interacting protein GTRAP3-18. *Nature* **410**, 84–88.

Liu SQ & Cull-Candy SG (2000). Synaptic activity at calcium-permeable AMPA receptors induces a switch in receptor subtype. *Nature* **405**, 454–458.

Liu SJ & Cull-Candy SG (2002). Activity-dependent change in AMPA receptor properties in cerebellar stellate cells. *J Neurosci* **22**, 3881–3889.

Liu SJ & Cull-Candy SG (2005). Subunit interaction with PICK and GRIP controls Ca2+ permeability of AMPARs at cerebellar synapses. *Nat Neurosci* **8**, 768–775.

Liu SJ & Lachamp P (2006). The activation of excitatory glutamate receptors evokes a long-lasting increase in the release of GABA from cerebellar stellate cells. *J Neurosci* **26**, 9332–9339.

Liu S, Lau L, Wei J, Zhu D, Zou S, Sun HS, Fu Y, Liu F & Lu Y (2004). Expression of Ca^{2+}-permeable AMPA receptor channels primes cell death in transient forebrain ischemia. *Neuron* **43**, 43–55.

Massey PV, Johnson BE, Moult PR, Auberson YP, Brown MW, Molnar E, Collingridge GL & Bashir ZI (2004). Differential roles of NR2A and NR2B-containing NMDA receptors in cortical long-term potentiation and long-term depression. *J Neurosci* **24**, 7821–7828.

Matsuda S, Mikawa S & Hirai H (1999). Phosphorylation of serine-880 in GluR2 by protein kinase C prevents its C terminus from binding with glutamate receptor-interacting protein. *J Neurochem* **73**, 1765–1768.

Momiyama A, Feldmeyer D & Cull-Candy SG (1996). Identification of a native low-conductance NMDA channel with reduced sensitivity to Mg^{2+} in rat central neurones. *J Physiol* **494**, 479–492.

Noh KM, Yokota H, Mashiko T, Castillo PE, Zukin RS & Bennett MV (2005). Blockade of calcium-permeable AMPA receptors protects hippocampal neurons against global ischemia-induced death. *Proc Natl Acad Sci U S A* **102**, 12230–12235.

Osten P, Khatri L, Perez JL, Kohr G, Giese G, Daly C, Schulz TW, Wensky A, Lee LM & Ziff EB (2000). Mutagenesis reveals a role for ABP/GRIP binding to GluR2 in synaptic surface accumulation of the AMPA receptor. *Neuron* **27**, 313–325.

Perez JL, Khatri L, Chang C, Srivastava S, Osten P & Ziff EB (2001). PICK1 targets activated protein kinase Calpha to AMPA receptor clusters in spines of hippocampal neurons and reduces surface levels of the AMPA-type glutamate receptor subunit 2. *J Neurosci* **21**, 5417–5428.

Petralia RS, Wang YX, Mayat E & Wenthold RJ (1997). Glutamate receptor subunit 2-selective antibody shows a differential distribution of calcium-impermeable AMPA receptors among populations of neurons. *J Comp Neurol* **385**, 456–476.

Sato K, Kiyama H & Tohyama M (1993). The differential expression patterns of messenger RNAs encoding non-*N*-methyl-D-aspartate glutamate receptor subunits (GluR1–4) in the rat brain. *Neuroscience* **52**, 515–539.

Scimemi A, Fine A, Kullmann DM & Rusakov DA (2004). NR2B-containing receptors mediate cross talk among hippocampal synapses. *J Neurosci* **24**, 4767–4777.

Seidenman KJ, Steinberg JP, Huganir R & Malinow R (2003). Glutamate receptor subunit 2 Serine 880 phosphorylation modulates synaptic transmission and mediates plasticity in CA1 pyramidal cells. *J Neurosci* **23**, 9220–9228.

Shen Y & Linden DJ (2005). Long-term potentiation of neuronal glutamate transporters. *Neuron* **46**, 715–722.

Song I & Huganir RL (2002). Regulation of AMPA receptors during synaptic plasticity. *Trends Neurosci* **25**, 578–588.

Srivastava S, Osten P, Vilim FS, Khatri L, Inman G, States B, Daly C, DeSouza S, Abagyan R, Valtschanoff JG, Weinberg RJ & Ziff EB (1998). Novel anchorage of GluR2/3 to the postsynaptic density by the AMPA receptor-binding protein ABP. *Neuron* **21**, 581–591.

Staudinger J, Zhou J, Burgess R, Elledge SJ & Olson EN (1995). PICK1: a perinuclear binding protein and substrate for protein kinase C isolated by the yeast two-hybrid system. *J Cell Biol* **128**, 263–271.

Thiagarajan TC, Lindskog M & Tsien RW (2005). Adaptation to synaptic inactivity in hippocampal neurons. *Neuron* **47**, 725–737.

Thompson CL, Drewery DL, Atkins HD, Stephenson FA & Chazot PL (2000). Immunohistochemical localization of N-methyl-D-aspartate receptor NR1, NR2A, NR2B and NR2C/D subunits in the adult mammalian cerebellum. *Neurosci Lett* **283**, 85–88.

Tovar KR & Westbrook GL (2002). Mobile NMDA receptors at hippocampal synapses. *Neuron* **34**, 255–264.

Tsvetkov E, Shin RM & Bolshakov VY (2004). Glutamate uptake determines pathway specificity of long-term potentiation in the neural circuitry of fear conditioning. *Neuron* **41**, 139–151.

Turecek R, Vlcek K, Petrovic M, Horak M, Vlachova V & Vyklicky L Jr (2004). Intracellular spermine decreases open probability of *N*-methyl-D-aspartate receptor channels. *Neuroscience* **125**, 879–887.

Washburn MS, Numberger M, Zhang S & Dingledine R (1997). Differential dependence on GluR2 expression of three characteristic features of AMPA receptors. *J Neurosci* **17**, 9393–9406.

Xia J, Chung HJ, Wihler C, Huganir RL & Linden DJ (2000). Cerebellar long-term depression requires PKC-regulated interactions between GluR2/3 and PDZ domain-containing proteins. *Neuron* **28**, 499–510.

Acknowledgements

This work was supported by a National Science Foundation grant (IBN-0344559) to S.J.L. We thank Philippe Lachamp, Yu Liu, Bernhard Luscher, Iaroslav Savtchouk and Matthew Whim for helpful discussions and comments on the manuscript.

Supplemental material

Online supplemental material for this paper can be accessed at:

http://jp.physoc.org/cgi/content/full/jphysiol.2007.136788/DC1

and

http://www.blackwell-synergy.com/doi/suppl/10.1113/jphysiol.2007.136788